Vacuum Breakdown on Metal Surfaces

Fred R. Schwirzke, *Member, IEEE*

Abstract— **Breakdown and plasma formation on surfaces are fundamental processes in many areas of pulsed power technology. The initial plasma formation on the surface of a cathode of a vacuum diode, vacuum arc, and many other discharges is highly nonuniform. Micron-sized cathode spots form within nanoseconds. The concept of explosive electron emission from a cathode spot is well established in the literature. However, the details of the breakdown process were not well understood. Unipolar arcing represents a discharge form which easily leads to explosive plasma formation. Power dissipation for an arc is considerably higher than for field-emitted or space-charge-limited current flow. Using a laser-produced plasma, it has been demonstrated that unipolar arcs ignite and burn on a nanosecond time scale without any external electric field being applied. Similar unipolar arc craters have now been observed on the cathode surface of a pulsed vacuum diode with an externally applied field of 0.5 MV/cm. The experimental results show that cathodes spots are formed by unipolar arcing. The localized buildup of plasma above an electron-emitting spot naturally leads to a pressure gradient and electric field distribution which drives the unipolar arc. The high current density of an unipolar arc provides explosive plasma formation.**

I. Introduction

MANY discharges form small cathode spots which provide such a high current density that the cathode material "explodes" into a dense plasma cloud within a very short time. Despite the fundamental importance of cathode spots for the breakdown process and the formation of a discharge, the complicated processes, the structure of the cathode spot, and the source of the high current density were not yet well defined, as the following citations from the literature show: "Processes in a cathode spot are extremely complicated and in many respects are still not understood" [2]; "Explosion of a microtip is accompanied by transition of the cathode matter into a dense plasma. The mechanism of this phase transition is not completely understood up to now" [3]; "At present, the mechanism of transport in the near-cathode region of a vacuum discharge is far from being revealed. There is a large discrepancy (up to three orders of magnitude) in experimental data on current density . . . . However (as far as we are aware), there is no paper that proposed a physical model that, at least qualitatively, describes with due regard for the dominant role of the explosion mechanism, and that explains the numerous experimental data from a single viewpoint" [4]; and "Cathode spots are complicated objects of both solid state physics and plasma physics. But on the plasma side, the experimental knowledge is rather scarce. More data is needed on the plasma dynamics . . . " [5]. Estimates of the current density j for a cathode spot vary by orders of magnitude between 10^5 A/cm^2 [1] and 10^9 A/cm^2 [2]. This is of critical importance, because the most significant parameters j and the electric field E determine field emission of electrons, joule heating, and plasma formation. Experimentally, j is measured by the electron flow between cathode and anode. In the prebreakdown phase, j is limited by the field-emission current density j_{FE} from an electron-emitting spot on the cathode surface such as a microprojection, adsorbed contaminant, metal grain boundary, etc. In short, a "whisker" may represent any electron-emitting spot where the field emission current is enhanced. During breakdown the exploding whisker forms the dense plasma, immediately above the electron-emitting spot [3]. The plasma surface then acts as a virtual cathode. The diode current density is now limited by the Child–Langmuir law for space-charge-limited currents j_{CL}. The Child–Langmuir current to the anode represents an upper limit, because $j_{FE} \ll j_{CL}$. For a diode voltage of 1 MV and a gap of $d = 1$ cm, assuming a uniform E, $j_{CL} = 2.3 \times 10^3$ A/cm^2, which is smaller than the $j \approx 10^8$–10^9 A/cm^2 required to explode a whisker by joule heating within a few nanoseconds. The field-emitted electron current will become space-charge-limited at a value which is insufficient for the explosive-like transition of the whisker into a dense plasma. The question then is how can the relatively small field-emission current lead to the "explosive" formation of a cathode spot within nanoseconds?

This paper describes the unipolar arc model and provides experimental proof that unipolar arcing [6] represents a discharge form which easily leads to explosive plasma formation. Due to its high current density, power dissipation for an arc is considerably higher than the one caused by field-emitted or space-charge-limited current flow.

The electron flow of the unipolar arc is from a "cathode" spot on the surface into the dense plasma cloud above the spot, and from the outer edges of the cloud back to the same surface in a ringlike "anode" area surrounding the cathode spot. Since both "electrodes" are located on the same metal surface, the arc is called "unipolar." The term *unipolar arc* was first introduced by Robson and Thoneman [7]. While their model describes essentially the electron return flow through the sheath, our model [6] elaborates upon the pressure gradient and the electric field distributions which are set up in the plasma and which derive the arc.

II. Onset of Vacuum Breakdown

The breakdown process in a vacuum diode is initiated by field emission of electrons from a cathode whisker or other

Manuscript received February 1, 1991; revised July 2, 1991. This work was supported by the Naval Research Laboratory, and by the Naval Postgraduate School.

The author is with the Department of Physics, Naval Postgraduate School, Monterey, CA 93943.

IEEE Log Number 9103160.

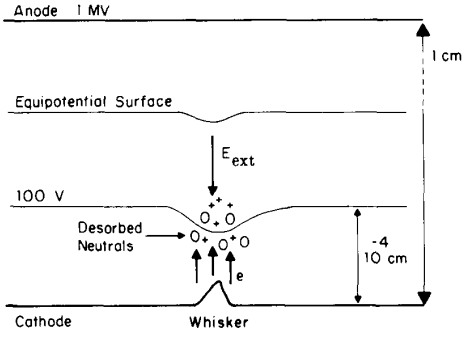

Fig. 1. Ionization of desorbed neutral particles near the 100-V equipotential surface where the ionization cross section has a maximum value.

emitting micropoints on the surface due to the externally applied electric field. In addition, since electrode surfaces are usually far from ultra high vacuum clean, the emission of electrons, the impact of ions, and the enhanced electric field stimulate desorption [8] of weakly bound adsorbates from the surface of the whisker. Expanding with sound velocity $v \approx 3.3 \times 10^4$ cm/s, a suddenly released monolayer of 2×10^{15} molecules/cm^2 forms a neutral gas layer. The average particle density of neutrals after 3 ns is $n_0 = (2 \times 10^{15}/\text{cm}^2)/vt = 2 \times 10^{19}$ cm^{-3}, with $vt = 10^{-4}$ cm. This neutral density produced by just one monolayer is almost atmospheric density. The electron mean-free-path length for ionizing neutrals $\lambda = 1/(n_0\sigma_0)$ depends on the ionization cross section σ_0, which in turn is a function of the electron energy. For many gases the ionization cross section has a broad maximum value of about $\sigma_0 \approx 10^{-16}$ cm^2 for electrons, with an energy between 50 to 150 eV. In an electric field of 10^6 V/cm, a field-emitted electron has gained 100 eV at the distance of 10^{-4} cm (Fig. 1). Thus $\lambda \approx 5 \times 10^{-4}$ cm and about 20% of the emitted electrons have a chance for an ionizing collision within $d \approx 10^{-4}$ cm. The probability for ionizing collisions increases with n_0; i.e., if several monolayers have been initially desorbed. For a diode, the onset of breakdown is typically delayed by 1 to 10 ns, which corresponds to the time of flight of the neutrals to the zone of maximum ionization; i.e., where the electrons have about 50 to 150 eV.

Ions produced at $d = 10^{-4}$ cm are accelerated back towards the electron-emitting spot. For an O_2^+ ions, the time of flight to the whisker surface would be 8×10^{-11} s, while the electrons would need a time of flight of 3.7×10^{-11} s to reach the anode 1 cm away. The positive ions produced at $d = 10^{-4}$ cm spend more time in front of the cathode. The buildup of positive space charge near the tip of the electron-emitting spot enhances E and j_{FE} (Fig. 2(a) and (b)). This will further increase the ionization rate and buildup of positive space charge. The ions arrive at the cathode surface with about 100 eV and recombine. The increasing ion bombardment and release of recombination energy lead to surface heating and further release of adsorbed gases [9] (discharge cleaning). The increasing positive space charge in front of the electron-emitting spot displaces the maximum ionization zone (where the electrons have about 100 eV) more closely to the cathode surface and into a region of higher neutral density. As the ionization rate further increases, a kind of double layer forms between the ions moving from the ionization zone to the cathode and the electrons moving to the anode. The electric field of the double

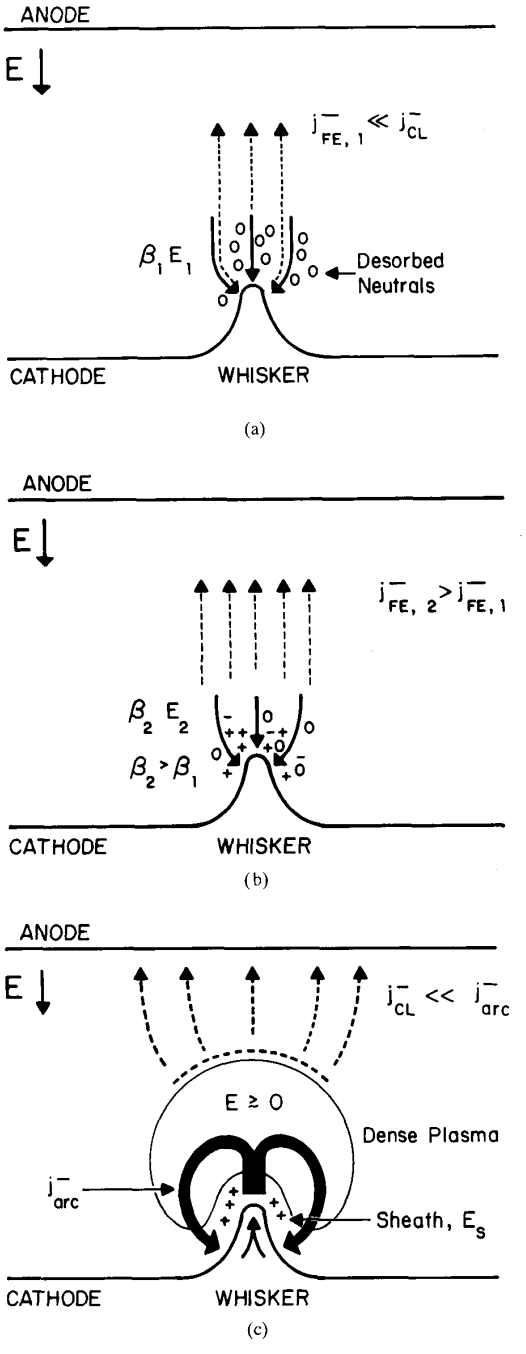

Fig. 2. (a) Field emission. (b) Enhanced field emission. (c) Sequence of events leading to the formation of a cathode spot by unipolar arcing. The dense plasma shields the cathode spot from the externally applied field E. j_{FE} = electron field mission current density; j_{CL} = electron Child–Langmuir space-charge-limited current density; β = electric-field-enhancement factor; and E_s = sheath electric field.

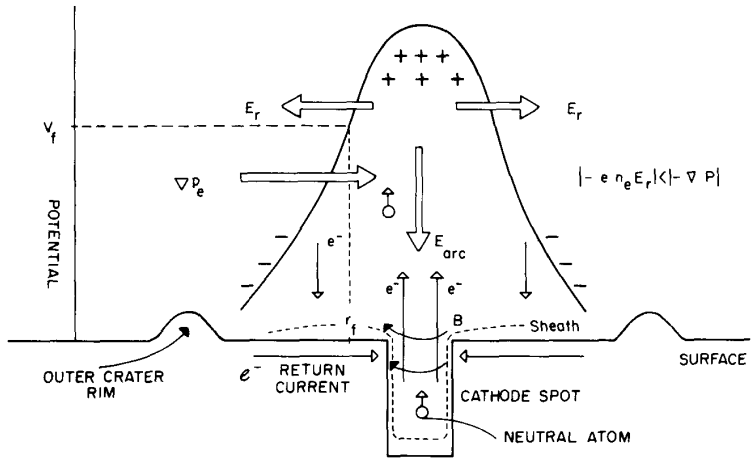

Fig. 3. Unipolar arc model.

layer reduces the external applied E_{ext} between the ionization zone and anode until the electron flow becomes space-charge-limited at j_{CL}. A plasma has formed that now screens E_{ext} from reaching the cathode. However, the plasma in "contact" with the cathode still forms a positive space-charge sheath of width given by $\lambda_d = \left(\epsilon_0 V_p / n_e e^2\right)^{1/2}$, where V_p is the plasma potential. The sheath electric field $E_s \approx V_p/\lambda_d$ controls now the electron emission. E_s approaches zero near the plasma boundary and assumes its maximal value at the surface. E_s ignites unipolar arcs. As the plasma density increases, so does the surface heating of the electron-emitting spot by ion bombardment. For the one-dimensional geometry considered up to now, the electron current to the anode is limited by j_{CL}. However, since the negative space charge associated with j_{CL} shields the plasma cloud from E_{ext}, the plasma electrons can flow sideways and even back to the cathode surface (Fig. 2(c)), as explained by the unipolar arc model.

Essentially, the same situation exists for a laser-produced plasma in contact with a metal surface. Without any external voltage being applied, the condition of quasi-neutrality for the laser-produced plasma in "contact" with the surface leads to the formation of a positive space-charge sheath with a width given by the Debye length λ_D and $E_s \approx V_f/\lambda_D$. The plasma assumes the positive floating potential V_f with respect to the surface given by:

$$V_f = \frac{kT_e}{2e} \ln\left(\frac{M_i}{2\pi m_e}\right), \qquad \lambda_D = \left(\epsilon_0 kT_e/e^2 n_e\right)^{1/2}. \quad (1)$$

The average electric field in the sheath is approximately:

$$E_s = \frac{V_f}{\lambda_D} = (n_e kT_e)^{1/2}(1/4\epsilon_0)^{1/2} \ln(M_i/2\pi m_e). \quad (2)$$

The sheath electric field increases with the local buildup of the plasma pressure as $E_s \propto P_e^{1/2}$.

III. Explosive Formation of Cathode Spots by Unipolar Arcing

Electron emission from a spot on the surface and desorption and ionization of adsorbates lead to the formation of a small dense plasma cloud about the electron-emitting spot. Since E_{ext} is screened from reaching the plasma, its dynamics is now determined by plasma pressure gradients, associated internal electric fields, and the sheath electric field. A sheath forms as the radially expanding plasma sweeps over the metal surface. The sheath potential distribution will be such that the quasi-neutrality of the plasma cloud is assured. The increasing plasma pressure P_e above the spot leads to a pressure gradient and an electric field E_r in radial direction, tangential to the surface (Fig. 3). Without any radial current flowing, this field would be the ambipolar electric field,

$$\vec{E}_{\text{amb}} = -\nabla P_e / e n_e. \quad (3)$$

Associated with this field, the plasma potential decreases in radial direction. Consequently, the plasma sheath potential is also reduced in a ring-like area A around the cathode spot. At some radial distance r_f from the cathode spot, the sheath potential will be equal to the floating potential (equation (1)), providing equal ion and electron flow rates to the surface at this location; i.e., the net current through the sheath is zero:

$$i_s = +en_i A\left(\frac{kT_e}{M_i}\right)^{1/2} - \frac{1}{4}|e| n_e \bar{v} A\left\{\exp\left(-\frac{|e|V_f}{kT_e}\right)\right\} = 0 \quad (4)$$

where $\bar{v}$ is the average speed of the electrons. The first term corresponds to the ion-saturation current which remains essentially constant, independent of the sheath potential for $V_s > 0$ (Fig. 4). The second term gives the electron flow through the sheath. At distances $r \lesssim r_f$, the plasma potential and thus the sheath potential $V_s \gtrsim V_f$ and the electron flow for a Maxwellian velocity distribution will change exponentially.

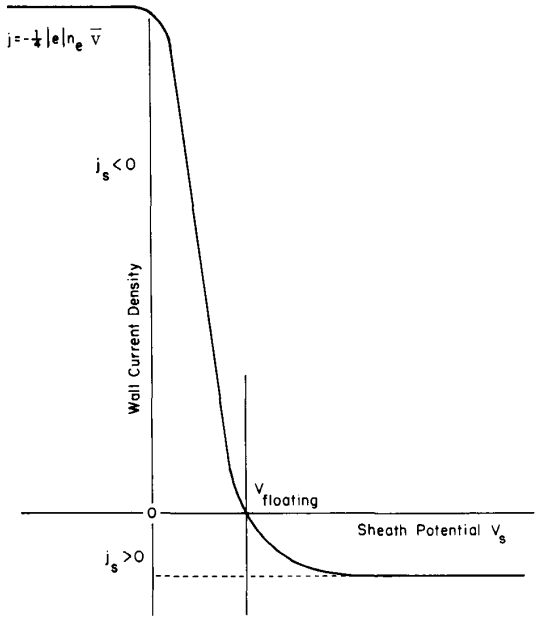

Fig. 4. Current density from the plasma to the wall as a function of the sheath potential V_s.

The net wall current density is then $j_s > 0$ for $V_s > V_f$, and $j_s < 0$ for $V_s < V_f$, while $j_s = 0$ for $V_s = V_f$.

$$j_s = -\frac{1}{4}\,|e|n_e\bar{v}\left\{\exp\left(-\frac{|e|V_s}{kT_e}\right) - \exp\left(-\frac{|e|V_f}{kT_e}\right)\right\}. \quad (5)$$

In this equation, the ion saturation current has been expressed by (4). $j_s > 0$ implies that more ions than electrons leave the plasma and the current is in the direction of the sheath electric field $\vec{E}_s$, from the positive plasma potential to the wall at zero potential. $j_s < 0$ means that more electrons than ions reach the wall. In the conventional sense, $\vec{j}_s$ is in the opposite direction to $\vec{E}_s$. At the front of the radially expanding plasma, V_s will approach zero; i.e., the radial potential drop ΔV from r_f to the outer edge of the plasma will be $\Delta V(r) \cong V_f$. From the radial pressure gradient (equation (3)), the amount of sheath reduction is found by integrating the radial electric field distribution, resulting in $\Delta V(r) = [kT_e/e]\ln[n_e(r_f)/n_{e0}]$. $n_e(r_f)$ is the plasma electron density at r_f, where $V_s = V_f$. $n_{e0}(r)$ is the plasma electron density at the outer edge. Equating ΔV with the sheaths floating potential (equation (1)),

$$\Delta V = V_f \quad \text{or} \quad \frac{kT_e}{e}\,\ln\,\frac{n_e(r_f)}{n_{e0}} = \frac{kT_e}{2e}\,\ln\,\frac{M_i}{2\pi m_e}$$

we find that independent of the electron temperature, the sheath potential can approach zero when:

$$\frac{n_e(r_f)}{n_{e0}} = \left(\frac{M_i}{2\pi m_e}\right)^{1/2}.$$

In this case, the electron return current to the surface is determined by the electron saturation current, $i_s = -(1/4)|e|n\bar{v}A$ (Fig. 4).

Actually, the increased flow of electrons to the surface at $r > r_f$ due to $V_s < V_f$ implies a reduction of the negative space charge. This results in a reduced radial electric field $E_r(r) = -\Delta V/\Delta r < E_{\text{amb}}$. Consequently, the outward-directed electron pressure gradient force becomes larger than the electric field force, which holds the electrons back $|-\nabla P_e| > \left|-en_e\vec{E}_r\right|$. A net force $\vec{F}_{\text{net}}$ acting on the electron fluid is pointing outward in the radial direction:

$$\vec{F}_{\text{net}} = -\nabla P_e - |e|n_e\vec{E}_r. \quad (6)$$

This is the driving force of the unipolar arc. The current density j of the arc follows from the equation of motion for the electron fluid,

$$-|e|n_e\vec{E}_r - \nabla P_e + |e|n_e\vec{j}/\sigma = 0.$$

The $j_r \times B_\Theta$ term has been omitted, because this term has no component in the radial direction. The $j_z \times B_\Theta$ component can lead to pinching of the arc axis. However, the collision frequency near the center of the metal vapor arc will be quite large. Estimates show that $\omega\tau < 1$ for magnetic fields $B < 1$ T. ω is the electron-cyclotron frequency, and τ, the time between collisions. For these reasons the influence of the arc magnetic field has been neglected in the present model of the unipolar arc.

σ is the electrical conductivity. The inertial term is assumed to be insignificant over the time scale of the arc. Solving for $\vec{j}$ and assuming a constant kT_e, independent of r, we find:

$$\vec{j} = \sigma\left(\frac{\nabla P_e}{en_e} - \frac{dV}{dr}\right) = \sigma\left(\frac{kT_e}{|e|n_e}\,\frac{dn_e}{dr} - \frac{dV}{dr}\right). \quad (7)$$

Again, $j = 0$ if the expression in the parentheses is zero; i.e., $-dV/dr = E_{\text{amb}}$.

It is essentially the mass difference between electrons and ions which causes a difference between the two terms on the right-hand side of (7). Due to the condition of quasi-neutrality, the plasma density profile is determined by the dynamics of the slow ions, $dn_e/dr = dn_i/dr$, while dV/dr is essentially determined by the more mobile electrons. From Poisson's law, it follows that small changes of the electron density lead to a change of the curvature of the potential curve,

$$\frac{d}{dr}\left(\frac{dV}{dr}\right) = \frac{|e|}{\epsilon_0}\,(n_e - n_i). \quad (8)$$

For a strictly one-dimensional density profile the curvature of the associated potential profile is proportional to $(n_e - n_i)$. It is concave downwards if $n_i > n_e$ (Fig. 5). At the location r_f, where $n_i = n_e$, $\left(d^2V/dr^2\right) = 0$. The curvature is concave upwards for $r > r_f$; i.e., $n_e > n_i$. In the two-dimensional geometry of the unipolar arc, the loss of electrons to the wall due to the reduced sheath potential $V_s < V_f$ in the region $r > r_f$ leads to a slight decrease of n_e by Δn_e. Consequently, the curvature will be reduced in this region:

$$\frac{d^2V}{dr^2} = \frac{|e|}{\epsilon_0}\,[(n_e - \Delta n_e) - n_i] > 0.$$

Still, $|n_e - \Delta n_e| > n_i$. The more pronounced curve in Fig. 5 schematically shows this change of the potential profile. As

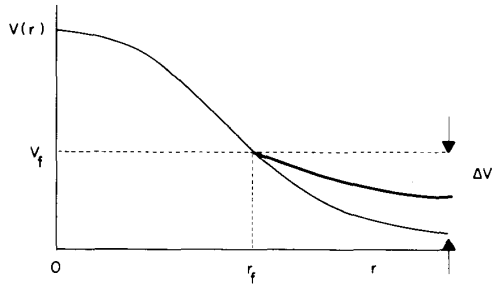

Fig. 5. Plot of plasma sheath potential as a function of the radial plasma dimension. The light curve is without electron losses to the surface; heavy curve is with electron losses. The electron-emitting cathode spot is at $r = 0$. r_f gives the location of the floating potential V_f.

more electrons flow from the plasma to the surface, $\Delta V(r)$ is decreased and the second term on the right-hand side of (7) $|dV/dr| < |(kT_e/en_e)(dn_e/dr)|$. Since $(dn/dr) < 0$, a $\vec{j} < 0$ results; i.e., $\vec{j}$ has the same sign as the current through the sheath $j_s < 0$ in the region $r > r_f$. $\Delta V(r)$ and the sheath potential $V_s(r)$ will adjust in the region $r > r_f$ to values which provide a continuous increasing current flow as more neutrals become ionized, thus increasing the driving ∇P_e term. The increasing temperature of the surface of the electron-emitting spot caused by ion bombardment and joule heating leads then to thermionic electron emission and a large arc current begins to circulate. This is the mechanism by which a cathode spot forms.

IV. Experiments

Using a laser-produced plasma, it has been demonstrated that unipolar arcs ignite and burn on a nanosecond time scale without any external voltage being present [10].

Laser-induced breakdown on surfaces was studied with a Q-switched neodymium laser of 25-ns FWHM. The laser pulse was directed onto targets placed in a vacuum chamber, providing pressures of the order of 10^{-6} torr. Incident laser energy was varied by inserting neutral density filters of varying transmittance in the beam path. For low-energy shots the laser amplifier was not fired. Laser energies on target between 0.0075 and 10 joules were obtained by these techniques. The beam was focused to various spot sizes on the target to provide further variation in power density. Low-power defocused laser pulses were used to study the onset of surface breakdown. A polaroid camera was positioned above the target to note plasma formation by recording the attendant light. Fig. 6 shows the damage on a stainless-steel surface once breakdown occurs, which is characterized by light emission from the plasma. The craters result from unipolar arcs burning between the plasma and surface. The hole at the center is the electron-emitting "cathode" of the arc; the surrounding ring with the crater rim is the electron-receiving "anode" area.

The craters are of various sizes. Longer burning arcs have larger outer rim diameters of up to 50 μm. Short burning arcs initiated towards the end of the laser pulse show a cathode hole of 0.5 to 1 μm diameter, with the formation of the outer

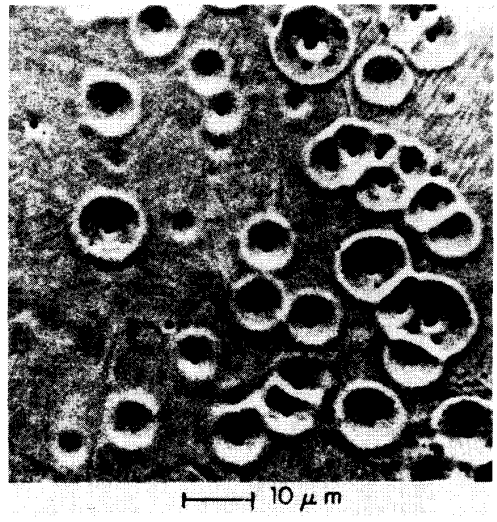

Fig. 6. Onset of laser-induced breakdown and unipolar arcing on stainless steel by a low-power unfocused laser pulse of 5.4 MW/cm^2.

crater rim just barely beginning. The depth of the cathode hole of 3–6 μm is larger than its diameter of about 1 μm. This indicates that the dense plasma or more specifically, the energy deposition by ion bombardment and joule heating drills the cathode hole. The material is ejected jet-like from this "hollow cathode" [11]. Small cathode holes have a diameter of about $\gtrsim$ 0.7 μm, which is smaller than the wavelength of the Nd laser, $\lambda = 1.06$ μm. Using the 10.6-μm radiation of a CO_2 laser, the same effect was observed—unipolar arc craters with cathode holes of $\sim$1 μm $\ll$ 10.6 μm, the laser wavelengths. This confirms that unipolar arcing is a plasma–surface interaction process and not a self-focusing effect.

A review of the target surface of Fig. 6 reveals that the damage is not evenly distributed. Besides the severe deformation caused by arcing, there is no other direct laser damage (like uniform surface melting) observable. All damage is in the form of arc craters. Cratering was observed even for defocused and low-power laser pulses. The power density threshold for the onset of breakdown and the onset of unipolar arcing is the same. The onset of arc damage is coincident with the onset of plasma formation. Never was there a plasma evident without attendant unipolar arcs. This leads to the conclusion that the initial breakdown process is represented by unipolar arcing.

In order to determine whether the vacuum diode breakdown mechanism is cathode spot formation via unipolar arcing, a Model 112A Pulserad generator was used with diode voltages between 0.84–1.1 MV, gap spacing of 2–2.5 cm, $E = 2.9$–5.8×10^5 V/cm, diode currents 14–21 kA, and a pulse length of 20 ns FWHM [12], [13]. The cathode was a stainless-steel cylindrical rod with a diameter of 3.18 cm. The cathode was repolished metallographically using a fine slurry of 0.05-μm Al_2O_3 after each shot. Characteristic unipolar arcing craters were observed on all exposed cathodes. However, as expected, the higher voltage shots displayed a greater density of craters and a higher degree of cathode surface

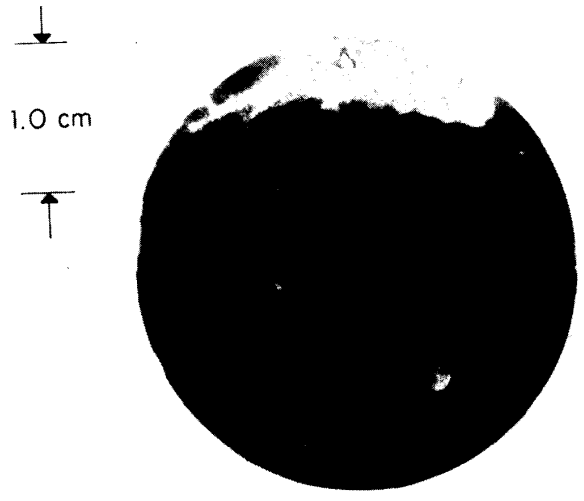

Fig. 7. Photograph of diode cathode surface after one discharge of 0.7 MV at a 1.91-cm gap spacing, $E = 3.7 \times 10^5$ V/cm, and a diode current of 14 kA.

melting than did the lower voltage shots. Fig. 7 shows the cathode surface after one low voltage shot. The dark area is the undamaged polished metal. The light areas are the sections of surface that underwent arcing. Overlapping unipolar arc craters are visible in the heavily damaged area (Fig. 8). Individual craters visible in Fig. 9 appear in the fringes of the light areas at the limit of the plasma formation. Grain boundaries are visible on the undamaged area. Again, as this figure shows, the primary damage visible (in the lightly damaged area of the cathode) is single unipolar arc craters on an otherwise undamaged surface. The first response to a high-voltage pulse is the formation of unipolar arcs on the cathode of the diode. This should be compared with Fig. 6, which is a close-up of laser-induced unipolar arcs on the surface of a stainless-steel target taken after one shot from a Neodymium laser of 25-ns FWHM with an average irradiance of 5.4 MW/cm^2. These figures and Figs. 10 and 11 show that the structure and size of the crater rim and cathode hole are essentially identical. As is the case for the laser-induced arcing, the craters on the cathode of the diode vary over a wide range.

V. Conclusions

Unipolar arcing can supply the necessary current density for explosive plasma formation and electron emission from a cathode surface spot in a nanosecond time frame. Unipolar arcing does occur on the surface of the cathode of a vacuum diode with the externally applied electric field, and it is remarkably similar to the interaction between a laser-produced plasma and a metal target surface with no external field. The following conclusions are also made:

- Unipolar arcing is the primary breakdown process leading to the formation of cathode spots.
- Surface breakdown is initiated by the ionization of desorbed contaminants by field-emitted electrons. Since this requires energy deposition only within a few contaminant monolayers at a time instead of an entire whisker volume, and since the neutral contaminants are only loosely bound to the surface by relatively weak Van der Waal forces, the onset of surface breakdown by this mechanism requires much less current and energy than vaporization and ionization of the entire cathode whisker. Since ion bombardment delivers more power to the whiskers than joule heating alone, the "explosive" transition of cathode

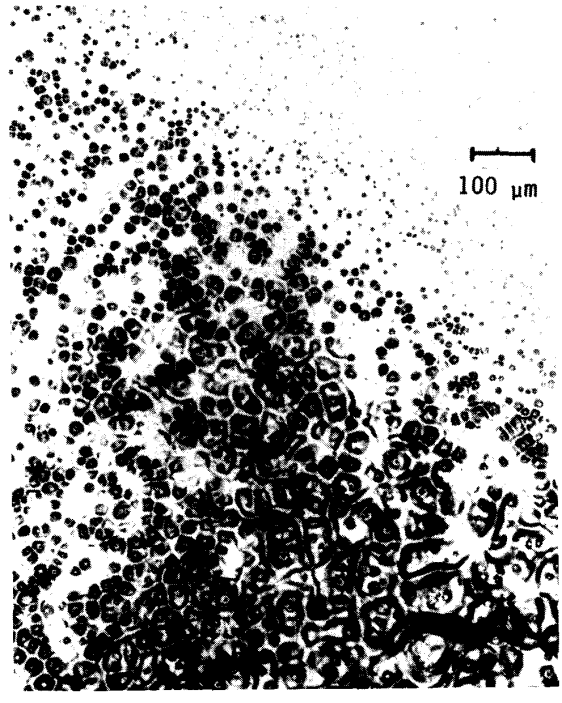

Fig. 8. Unipolar arc craters near the edge of the heavily damaged area of the cathode of Fig. 7. Single small craters can be seen in the upper right-hand corner (Fig. 9).

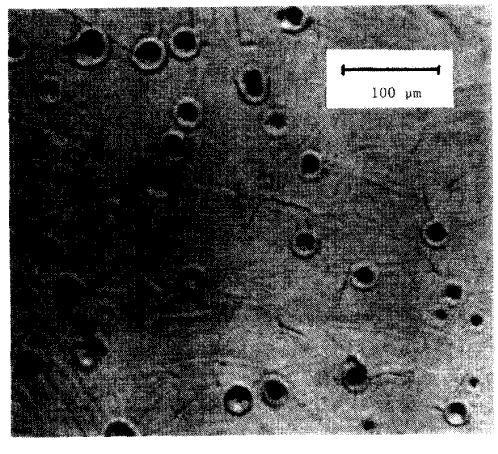

Fig. 9. Crater formation on the cathode of diode.

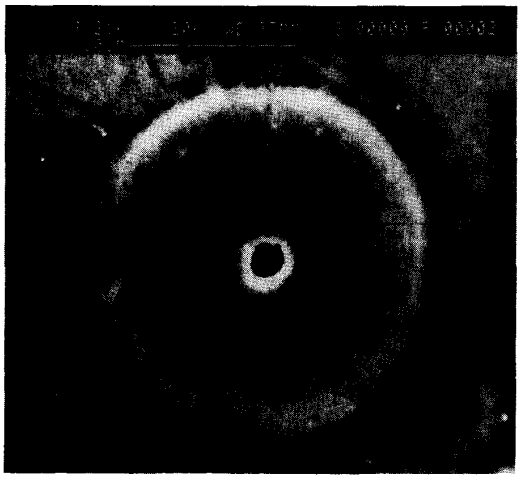

Fig. 10. Unipolar arc crater on the cathode surface.

Fig. 11. Laser-produced arc crater. Rim-to-rim diameter is 5.5 μm, and the cathode spot size is 0.7 μm.

material into plasma can occur at unipolar arc current densities, $j \ll 10^9$ A/cm^2.

- The localized buildup of plasma above an electron-emitting spot naturally leads to pressure and electric field distributions which cause unipolar arcing.
- Since the external field is screened from the cathode surface, the whisker current is no longer determined by the space-charge-limited current. Hence the unipolar arc current density can be many order of magnitude greater than the Child–Langmuir space-charged-limited diode current density.
- The large variation in published values for cathode spot current densities can be explained by the fact that the unipolar arc current is not included in measurements of the overall diode current density.
- The closure of the diode gap results from the expansion of the plasma ions under the influence of the plasma pressure gradient. This can occur, since the external electric field is effectively screened from the dense plasma when the current to the anode becomes space-charge-limited. The ions thus see no retarding external field.
- Unipolar arcing represents a basic form of a small-scale discharge which contributes to phenomena-like laser-induced breakdown and formation of cathode spots in a unique way.

REFERENCES

[1] V. I. Rakhovsky, *IEEE Trans. Plasma Sci.*, vol. PS-12, p. 199, 1984.
[2] E. A. Litvinov, G. A. Mesyats, and D. I. Proskurovski, *Sov. Phys. Usp.*, vol. 26, p. 138, 1983.
[3] G. N. Fursey, *IEEE Trans. Elec. Insul.*, vol. EI-20, p. 659, 1985.
[4] V. I. Rakhovsky, *IEEE Trans. Plasma Sci.*, vol. PS-15, p. 481, 1987.
[5] B. Jüttner, *IEEE Trans. Elec. Insul.*, vol. EI-20, p. 659, 1985.
[6] F. Schwirzke, *J. Nucl. Mat.*, vols. 128 and 129, p. 609, 1984.
[7] A. E. Robson and P. C. Thonemann, *Proc. Phys. Soc.*, vol. 73, p. 508, 1959.
[8] J. Halbritter, *IEEE Trans. Elec. Insul.*, vol. EI-18, p. 253, 1983; see also, *IEEE Trans. Elec. Insul.*, vol. EI-20, p. 671, 1985.
[9] F. Schwirzke, H. Brinkschulte, and M. Hashmi, *J. Appl. Phys.*, vol. 46, p. 4891, 1975.
[10] F. Schwirzke, "Laser-induced unipolar arcing," in *Laser Interaction and Related Plasma Phenomena*, vol. 6, H. Hora and G. H. Miley, Eds. New York: Plenum, 1984, pp. 335–352.
[11] F. Schwirzke, "Plasma jets emitted by unipolar arcing from spherical laser targets," in *Laser Interaction and Related Plasma Phenomena*, vol. 7, H. Hora and G. H. Miley, Eds. New York: Plenum, 1986, pp. 843–855.
[12] S. A. Minnick, "Unipolar arcing on the cathode surface of a high voltage diode," M. S. thesis, Naval Postgraduate School, Dec. 1989.
[13] F. Schwirzke, X. K. Maruyama, and S. A. Minnick, *Bull. Amer. Phys. Soc.*, vol. 34, p. 2103, 1989.

Fred R. Schwirzke (M'78) received the degree Dr. rer. nat. from the University Karlsruhe (Germany) in 1959.

From 1959 to 1962 he worked at the Max Planck Institute for Physics and Astrophysics, Munich, and at the Institute for Plasma Physics, Garching, Germany. From 1962 to 1967 he was a staff member of the plasma physics group at General Atomic, San Diego, CA. He performed research on plasma diffusion, plasma sheath effects, and laser-produced plasmas. Since 1967 he has been on the faculty of the Naval Postgraduate School, where he is presently Professor of Physics. His research interests are in the areas of plasma surface effects, magnetic field generation in laser-produced plasmas, and shock waves and breakdown phenomena.